Electronic Supplementary Material (ESI) for RSC Advances

Supporting Information for

Phase Behavior of Mesoporous Nanostructures Templated by Amphiphilic Crystalline–Crystalline Diblock Copolymers of Poly(ethylene oxide-*b*-ε-caprolactone)

Jheng-Guang Li, and Shiao-Wei Kuo*

Department of Materials and Optoelectronic Science, Center for Nanoscience and Nanotechnology, National Sun Yat-Sen University, Kaohsiung, 804, Taiwan

*To whom corresponding should be addressed

E-mail: kuosw@faculty.nsysu.edu.tw

TEL: 886-7-5252000 ext.4079

FAX: 886-7-5254099

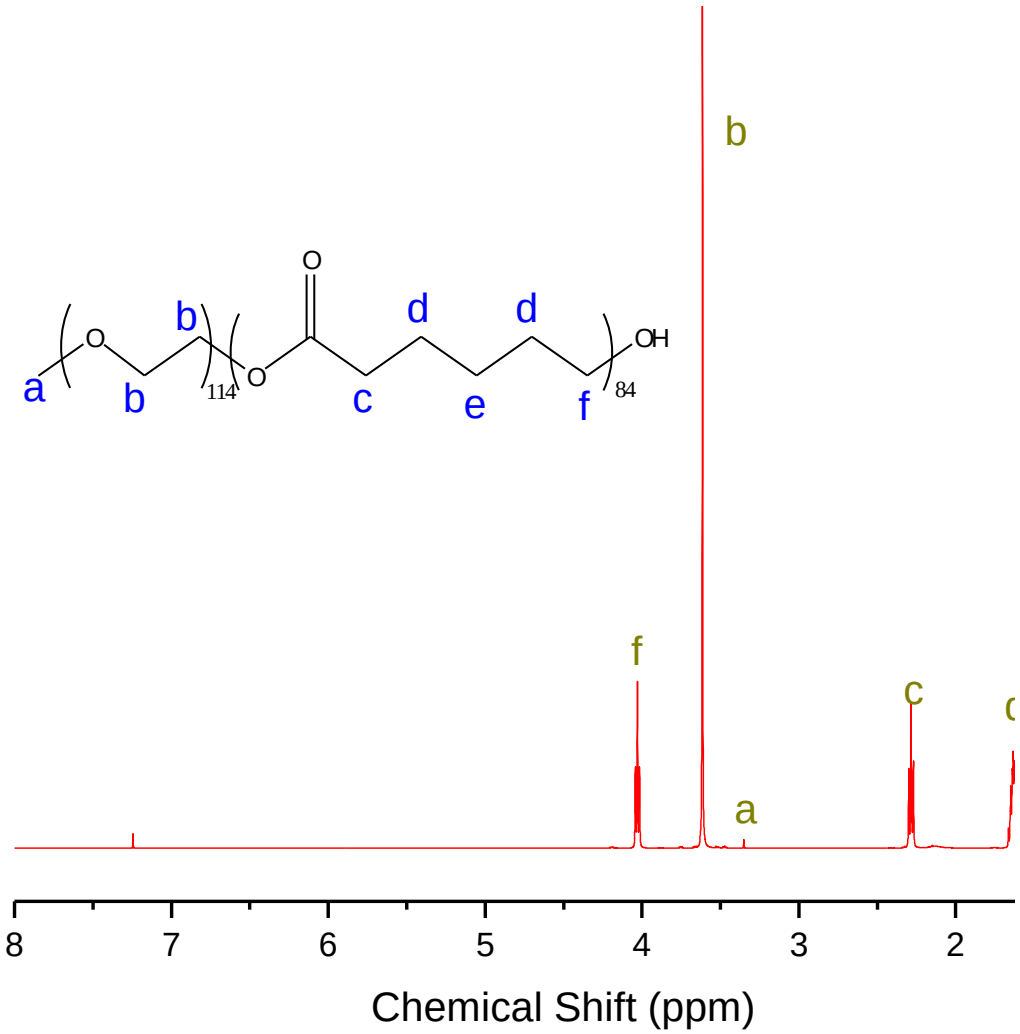

Figure S1: ^{1}H NMR of PEO-*b*-PCL copolymer (in $CDCl_3$)

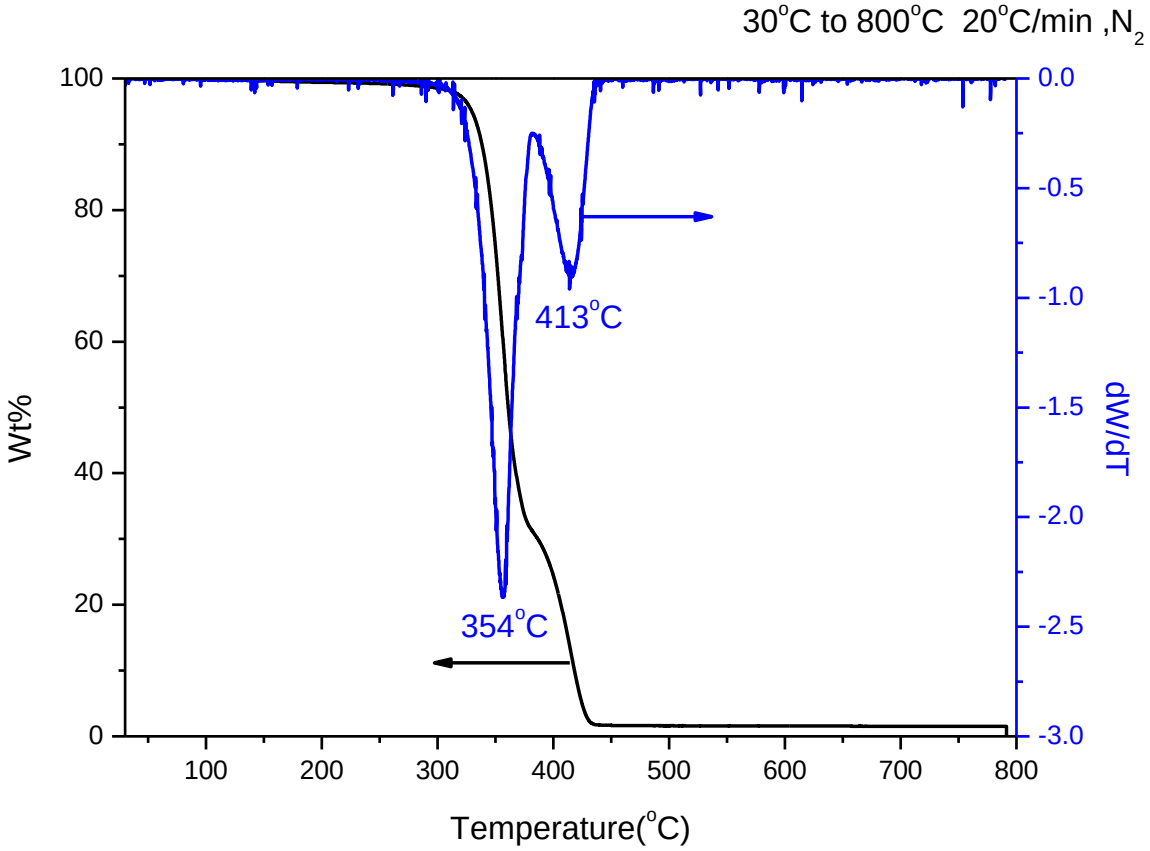

Figure S2: TGA analysis of PEO-b-PCL block copolymer under nitrogen.

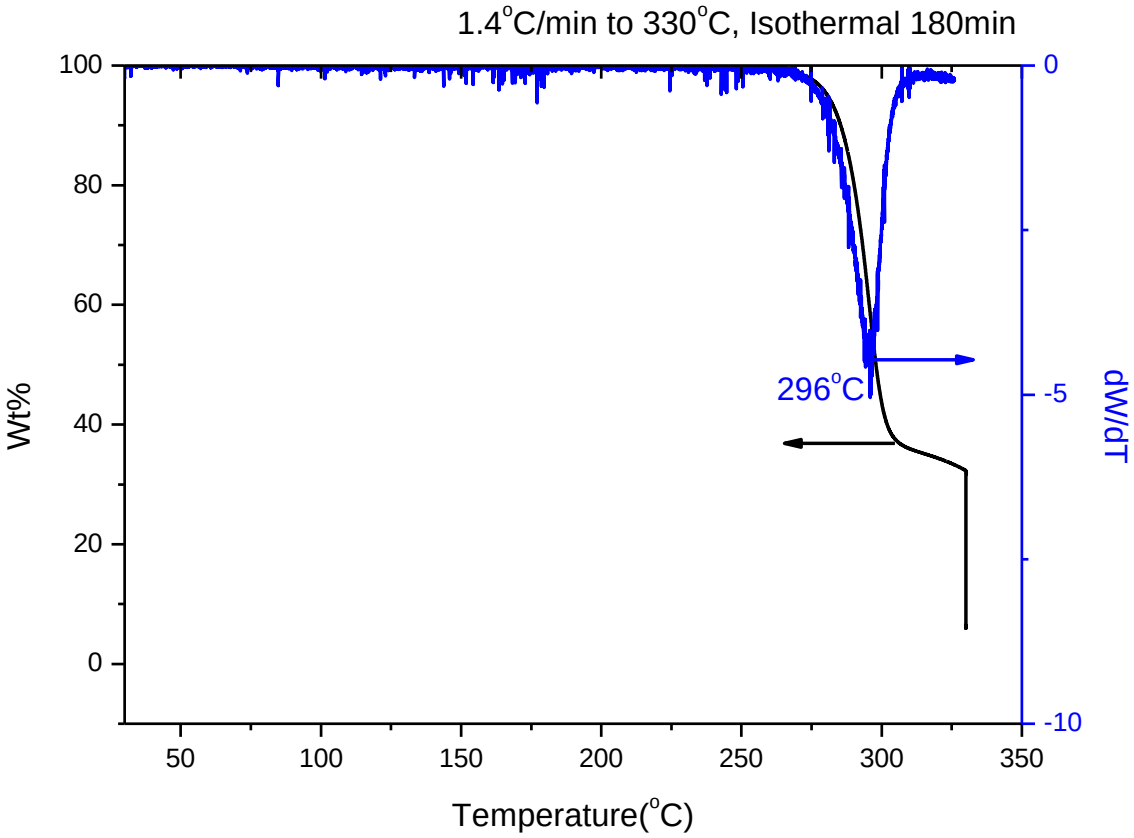

Figure S3: TGA analysis of PEO-b-PCL block copolymer under air

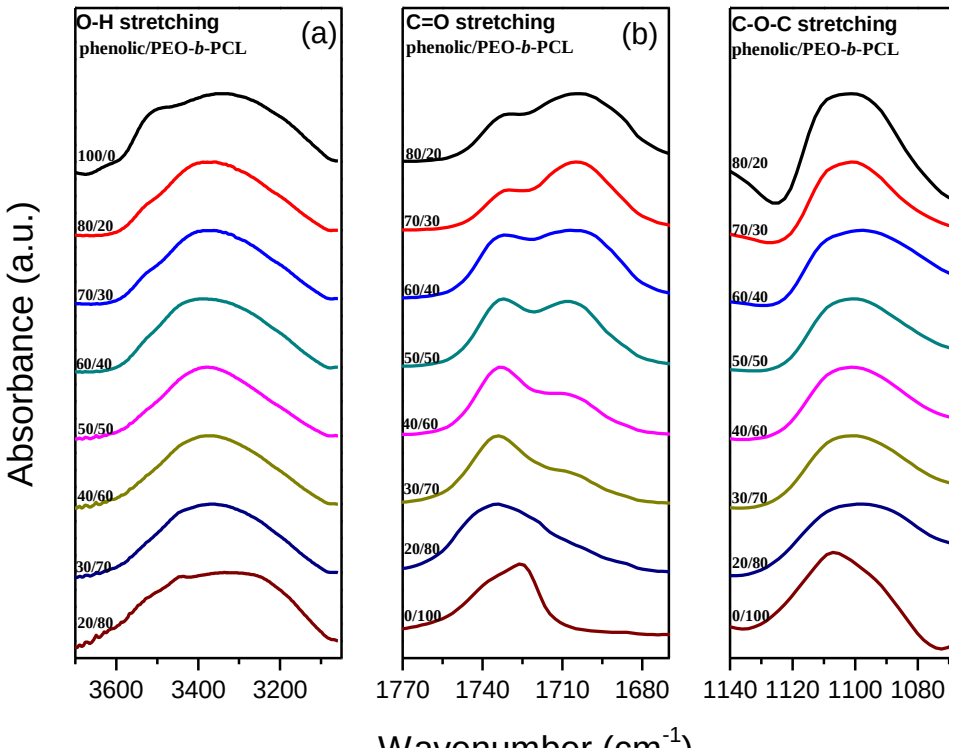

Figure S7. FT-IR spectra at room temperature of the phenolic/PEO-*b*-PCL blend displaying the (a) hydroxyl, (b) carbonyl and (c) ether region

Table S1: Curve-fitting result of phenolic/PEO-b-PCL blend at room temperature

	Free C=O			H-Bonded C=O		
PEO-*b*-PCL /Phenolic	v (cm^{-1})	$W_{1/2}$ (cm^{-1})	A_a (%)	v (cm^{-1})	$W_{1/2}$ (cm^{-1})	A_b (%)
80/20	1735	23	76.3	1709	26	23.7
70/30	1734	23	64.4	1709	26	35.6
60/40	1734	22	58.7	1708	28	41.3
50/50	1734	22	42.1	1707	28	57.9
40/60	1734	22	29.3	1706	30	70.7
30/70	1733	20	20.1	1705	30	79.9
20/80	1734	20	18.4	1704	30	81.6

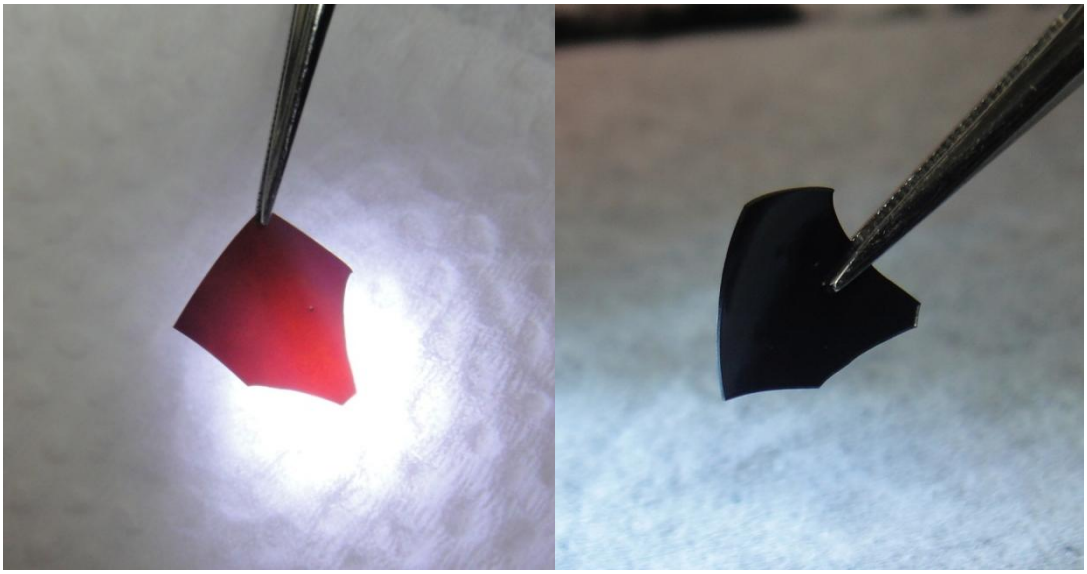

(a) (b)

Figure S5: Photographed images of (a) phenolic/PEO-*b*-PCL = 50/50 blend, and (b) mesoporous phenolic resin after calcination from (a).

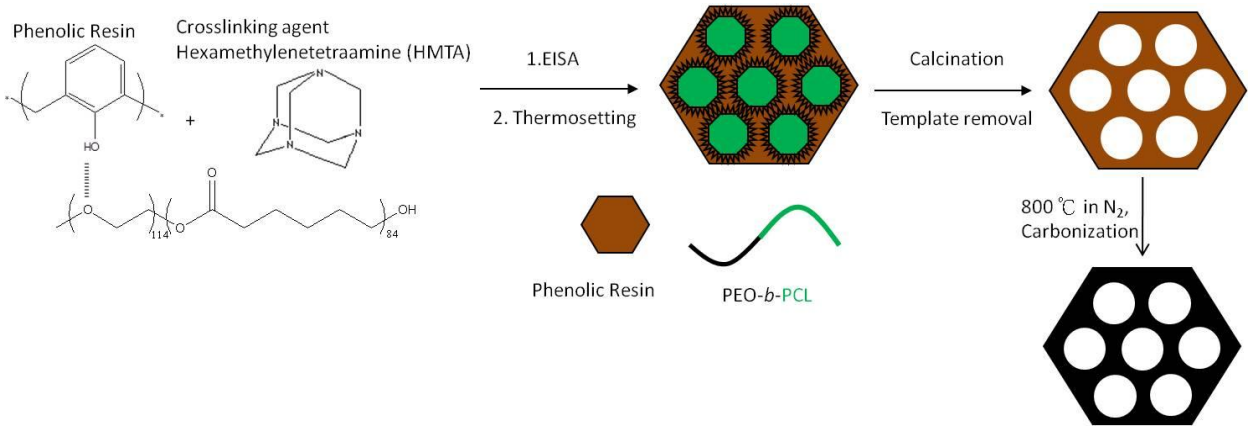

Scheme S1: Preparation of mesoporous carbon

Phase behavior of mesoporous carbon

Figure S6 displays the SAXS pattern and TEM images of gyroid mesoporous carbon pyrolyzed from mesoporous phenolic resin (phenolic-*c*). Figure S5(a) presents the set of Bragg reflections with an approximate relative q values of $6^{1/2}q^*$, $20^{1/2}q^*$, and $38^{1/2}q^*$, corresponding to a gyroid ($Ia\bar{3}d$)structure. This pattern is the same with gyroid phenolic resin (phenolic-*c*), where a large unit of *d*-spacing is calculated to be 23.6 nm (Table 1). Furthermore, the well-resolved SAXS pattern is

retained, indicating that the highly ordered mesostructure of the mesoporous carbon is thermally stable after calcination at 800 °C in N_2. The *d*-spacing is as large as 18.6 nm of mesoporous carbon, reflecting 21% shrinkage of the polymer framework. Figures S6b, c, and d show display TEM images and corresponding Fourier diffractograms, indicating that the mesoporous carbon has a high degree of periodicity over large domains. This result is viewed from the [110], [311], and [111] directions from the gyroid phenolic resin calcined at 800 °C under N_2.

Figure S7 shows the texture of the mesoporous carbon characterized by N_2 physisorption experiments and the corresponding N_2 adsorption–desorption isotherms and pore size distributions. We observed that the gyroid carbon was also a typical mesoporous material. In Figure S6A, the gyroid carbon exhibited representative type IV isotherms with H_1 hysteresis loops, according to IUPAC classification.[80] These isotherms suggested that the uniform, large, cylindrical pores were retained. Furthermore, sharp steps occurred at relative pressures of 0.45 to 0.85 for this sample, indicating a full filling of the uniform mesopores from the capillary force. Compared to the gyroid mesoporous phenolic resin (phenolic-*b*), the mean pore size measured from the adsorption branch was decreased to 11.0 nm, as shown in Figure S6B and Table 1. The BET surface area and pore volume were 858 m^2/g and 0.59 cm^3/g, respectively (Table 1). The BET surface area was much larger than that of the gyroid mesoporous phenolic resin. The result was due to the continuous removal of carbon, hydrogen, and oxygen from the mesoporous matrix during pyrolysis. The *t*-plot calculation revealed that the micropore surface area of the mesoporous carbon was 647 m^2/g, which was much larger than that of the mesoporous phenolic resin. The process primarily introduced the micropores, demonstrating that micropores are generated during the carbonization.

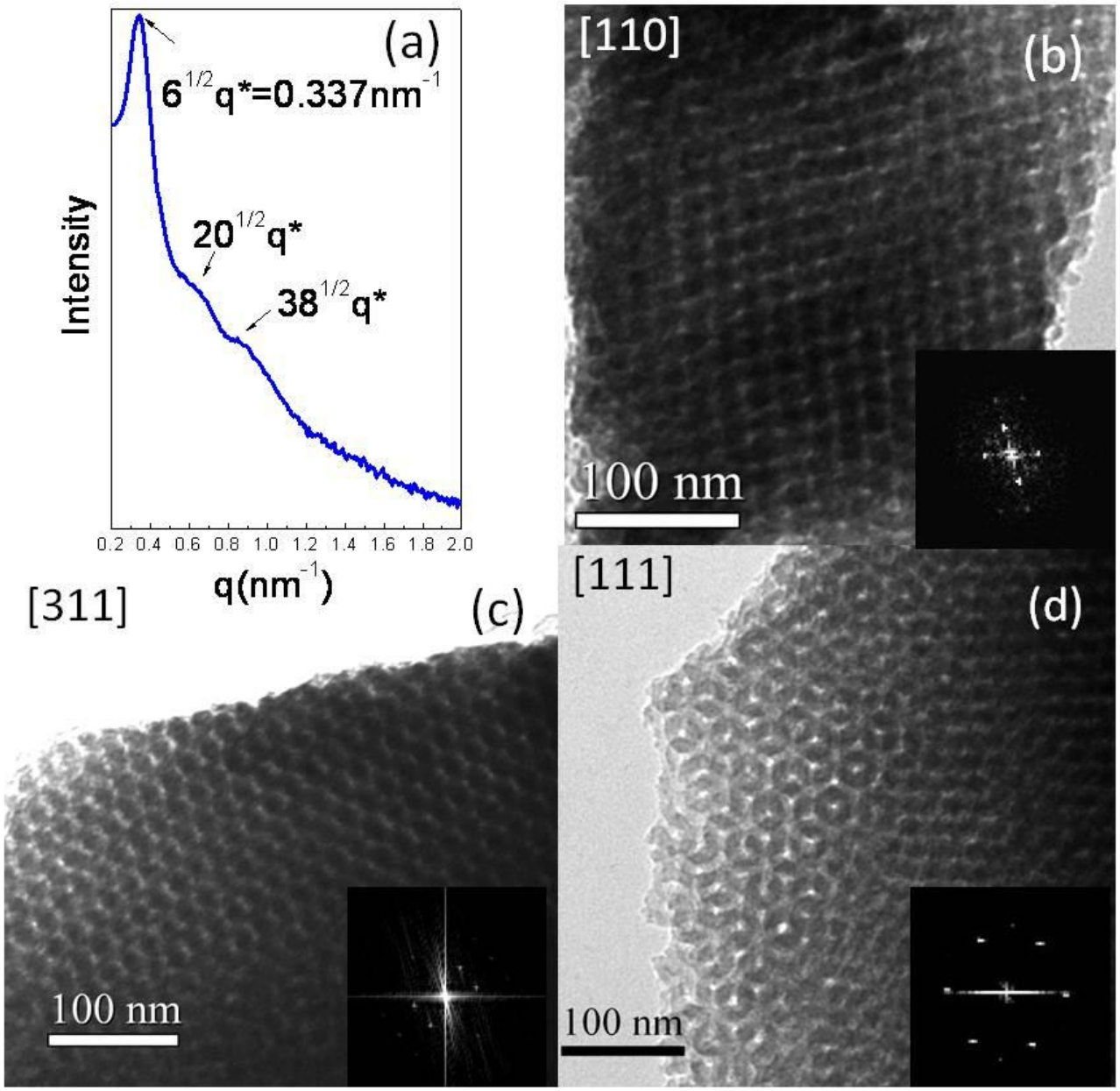

Figure S6. SAXS pattern and TEM images of gyroid mesoporous carbon pyrolyzed from mesoporous phenolic resin (phenolic-*b*) at 800 °C.

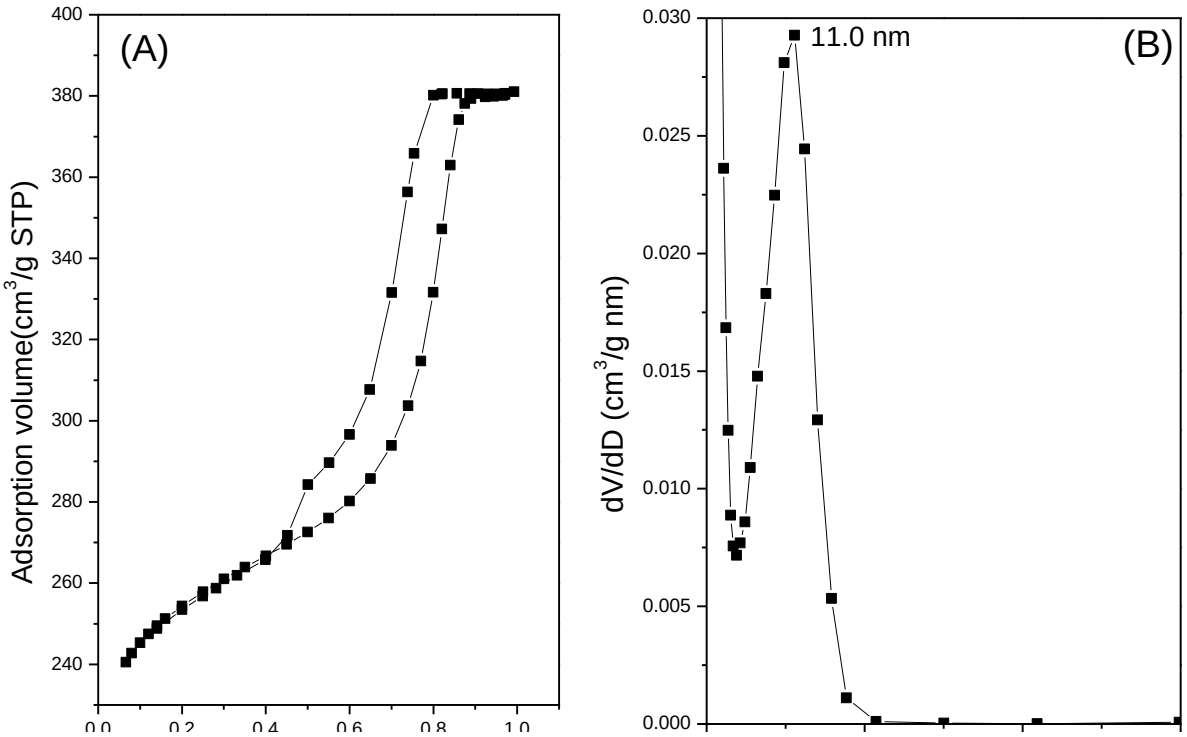

Figure S7. (A) N_2 adsorption-desorption isotherms and (B) pore size distribution curves of mesoporous carbon pyrolyzed at 800° C in N_2, weight fraction (phenolic resin/ $EO_{114}CL_{84}$ =50/50)